Gold nanoparticles electrodeposited on glassy carbon using cyclic voltammetry: Application to Hg(II) trace analysis

Teddy Hezard [a,b,c,d], Katia Fajerwerg [e,f,*], David Evrard [a,*], Vincent Collière [e,f], Philippe Behra [b,c], Pierre Gros [a]

[a] Université de Toulouse, Laboratoire de Génie Chimique, UMR CNRS/INPT/UPS 5503, Université Paul Sabatier, F-31062 Toulouse CEDEX 9, France
[b] Université de Toulouse, INPT, LCA (Laboratoire de Chimie Agro-industrielle), UMR 1010, ENSIACET, 4 allée Emile Monso, F-31030 Toulouse CEDEX 4, France
[c] INRA, LCA (Laboratoire de Chimie Agro-industrielle), F-31030 Toulouse, France
[d] FCS RTRA "Sciences et Technologies pour l'Aéronautique et l'Espace", 23 avenue Edouard Belin, F-31400 Toulouse, France
[e] CNRS, LCC (Laboratoire de Chimie de Coordination), 205 route de Narbonne, F-31077 Toulouse, France
[f] Université de Toulouse, UPS, INPT, LCC, F-31077 Toulouse, France

Keywords:
Hg(II) trace analysis
Gold nanoparticles
Modified electrodes
Electrodeposition
Cyclic voltammetry

A B S T R A C T

The electrochemical determination of Hg(II) at trace level using gold nanoparticles–modified glassy carbon (AuNPs–GC) electrodes is described. Starting from $HAuCl_4$ in $NaNO_3$, gold nanoparticles (AuNPs) were deposited onto Glassy Carbon (GC) electrodes using Cyclic Voltammetry (CV). Different deposits were obtained by varying the global charge consumed during the whole electroreduction step, depending on the number of cyclic potential scans (*N*). AuNPs were characterized as a function of the charge using both CV in H_2SO_4 and Field Emission Gun Scanning Electron Microscopy (FEG-SEM). The AuNPs–GC electrodes were then applied to determine low Hg(II) concentrations using Square Wave Anodic Stripping Voltammetry (SWASV). The AuNPs–GC electrodes provided significantly improved performances in Hg(II) determination compared to unmodified GC and bare Au electrodes. It was shown that the physico-chemical properties of the deposits are correlated to the performances of the AuNPs–GC electrode with respect to Hg(II) assay. The best results were obtained for four electrodeposition cyclic scans, where small-sized particles (36 ± 13 nm) with high density (73 particles μm^{-2}) were obtained. Under these conditions, a linearity range from 0.64 to 4.00 nM and a limit of detection of 0.42 nM were obtained.

1. Introduction

Heavy metal ions constitute a major problem with respect to environment and healthiness not only because they are widely distributed in natural systems such as atmosphere, water or soil, but also due to the great hazard they represent towards living organisms [1,2]. Amongst them, Hg and its speciation appear to be one of the highest priority targets since its strong affinity for biological compounds emphasizes its toxicity [3]. Hg(II) compounds, and particularly mono- and di-methylmercury, accumulate in vital organs and tissues and are responsible for chronic diseases, kidney injury, respiratory failure, central nervous system disorders, brain damages, and can even also induce death [4,5]. Thus, Hg(II) analysis, quantification and speciation in the environment is one of the most challenging research field for analytical chemists aiming at environmental survey, and there is an increasing need for systems that deliver rapid and reliable data. Moreover, bioaccumulation phenomena make Hg(II) dangerous even at very low concentration [6–10]. A particular effort has thus to be made in order to enhance the sensitivity and to reduce detection limits of such analytical devices.

Many spectroscopic techniques are reported in the literature that offer selectivity and quite good sensitivity with respect to Hg(II) trace determination, such as Cold Vapor Atomic Absorption Spectroscopy (CVAAS), Cold Vapor Atomic Fluorescence Spectroscopy (CVAFS) and Inductively Coupled Plasma Mass Spectrometry (ICP-MS) [11]. Although these techniques allow very low concentrations to be determined, they all involve expensive material and require complicated procedures. Consequently they are not really suitable for *in situ* or on line and *operando* analysis.

Comparatively, electrochemical sensors are cheap and portable devices with simple procedures and low energy requirement that can be used either in laboratory or for on-site measurements. Many electrochemical techniques are used for Hg(II) determination, such as potentiometry [12], chronopotentiometry [13] and pulsed amperometry [14], the most commonly used being Differential

* Corresponding authors. Addresses: CNRS, LCC (Laboratoire de Chimie de Coordination), 205 route de Narbonne, F-31077 Toulouse, France. Tel.: +33 (0)5 61 33 31 30; fax: +33 (0)5 61 55 30 03 (K. Fajerwerg); Université de Toulouse, Laboratoire de Génie Chimique, UMR CNRS/INPT/UPS 5503, Université Paul Sabatier, F-31062 Toulouse CEDEX 9, France. Tel.: +33 (0)5 61 55 60 73; fax: +33 (0)5 61 55 61 39 (D. Evrard).

E-mail addresses: Katia.Fajerwerg@lcc-toulouse.fr (K. Fajerwerg), evrard@chimie.ups-tlse.fr (D. Evrard).

Pulse Voltammetry (DPV) [15,16] and Square Wave Voltammetry (SWV) [17–19]. Moreover, the combination of a preconcentration step like Anodic Stripping Voltammetry (ASV) [20] with those pulsed techniques allows detection limits in the picomolar range to be reached [15,18].

Many working electrode materials have also been tested, such as platinum [21], graphite [22], Glassy Carbon (GC) [16,23,24], carbon paste [25], multi-walled carbon nanotubes [26,27], cylindrical carbon fiber [28] and gold. Because of its strong affinity for Hg that enhances the preconcentration effect during the accumulation step, this latter is the most commonly used electrode material. A rapid glance to the literature offers a good insight of the wide range of such systems that have been reported: Au can be used as a bulk [15,17,29], film [30,31], microwire [18,32], microdisk [33], or microdisk array electrode [34].

Another strategy that is frequently encountered to improve the performances of the electrochemical sensor is to chemically modify electrode: the electroactive surface is then functionalized using either polymers [35,36], organic [37] or biological compounds [38,39] chosen for their complexing affinity towards Hg(II).

During the last two decades, interests have focused on nanoscaled materials and their use in analytical chemistry because of their specific physico-chemical properties for a wide range of applications including electronics, optics, catalysis and biological sensors. Improvements resulting from metal nanoparticles for electroanalysis are numerous: sensing interface roughening, catalytic and conductive properties, and mass transport enhancement [40]. These attractive properties combined to the strong affinity of Au for Hg favoured the appearance of a new kind of electrode modification involving Au nanoparticles (AuNPs) [40,41]. AuNPs can be prepared by chemical synthesis [42,43] or by physical ways such as magneton sputtering, radiolytic and photolytic methods [44,45]. Electrodeposition provides a complementary easy, rapid and cheap alternative [46,47]. Most electrodeposited monometallic AuNPs-based electrodes have been used as gas sensors and for bioanalytical purposes. In comparison their application for ASV of metalloids and trace metals such as As(III) or Hg(II) is less explored [46,48]. To the best of our knowledge, Hg(II) trace determination on such monometallic AuNPs-based electrodes is limited to Gao et al. [49] and more recently to Abollino et al. [48] studies. In both cases AuNPs were electrodeposited by chronoamperometry on Au or GC electrode respectively. In the present work, Cyclic Voltammetry (CV) was used for AuNPs electrodeposition onto GC electrodes. This method was preferred for several reasons: it is indicative of the occurrence of adsorption phenomena either of the reactant or the product, and gives also insight of the presence of intermediates in the Au(III) reduction mechanism. The relative importance of mass transfer phenomena *vs*. heterogenous electron transfer can be discriminated. Moreover, the shape of the cyclic voltammograms is characteristic of nucleation and growth processes [50,51]. Finally, CV enables the determination of the optimal conditions for AuNPs electrodeposition (potential range, $AuCl_4^-$ concentration, etc.).

Despite the work by Gong et al. [52] that reported bimetallic Au–Pt nanoparticles deposited onto organic nanofibers on a GC electrode using CV, this paper presents for the first time a study concerning monometallic AuNPs electrodeposition on GC electrodes by CV aiming at Hg(II) trace detection using Square Wave Anodic Stripping Voltammetry (SWASV). The amperometric response of the modified electrode was examined as a function of the number of electrodeposition cyclic scans (N) and correlated to the AuNPs size and density determinated by Field Emission Gun Scanning Electron Microscopy (FEG-SEM). Finally the sensitivity of the resulting sensor towards Hg(II) assay was evaluated and compared to those recorded on bare Au and unmodified GC electrodes.

2. Experimental

2.1. Chemicals and apparatus

All the solutions were prepared using ultra pure water (Milli-Q, Millipore, 18.2 MΩ cm). $HAuCl_4{\cdot}3H_2O$ (pro analysis grade) was purchased from Acros Organics. $NaNO_3$ and HCl 30% (suprapur grade) were obtained from Merck. H_2SO_4 95% (normapur grade) was supplied by VWR Prolabo. A standard stock solution of 4.99 ± 0.01 μM Hg(II) was prepared by dilution of 1001 ± 2 mg L^{-1} $Hg(NO_3)_2$ NIST standard solution (certiPUR grade, Merck) and acidified to pH 2 with concentrated HNO_3 65% (suprapur grade, Merck), and then used as is for further dilution.

All the electrochemical experiments were performed at room temperature in a Teflon PFA three-electrode cell (Metrohm) by using a PGSTAT 128N potentiostat (Metrohm Autolab, Utrecht, Netherlands) interfaced to a laptop computer and controlled with NOVA 1.7 software package (Metrohm). A Metrohm Ag/AgCl/KCl 3 M electrode, separated from the electrochemical cell by a Teflon PTFE capillary containing a 0.1 M $NaNO_3$ solution and terminated by a ceramic diaphragm (D type), and a Metrohm GC wire were used as reference and counter electrodes, respectively. Working electrodes were rotating disk electrodes from Radiometer, either in GC (3 mm diameter, $A = 7.07\ mm^2$), Au (2 mm diameter, $A = 3.14\ mm^2$) or AuNPs–modified GC (AuNPs–GC). The electrochemical cell was constantly maintained in a Faraday cage in order to minimize the electrical interferences. When indicated, the solutions were deaerated using a N_2 stream for 10 min. A N_2 atmosphere was then maintained over the solution during the corresponding experiments.

2.2. Electrode preparation and modification

Prior to each modification, the GC surfaces were polished successively by silicon carbide grinding paper (grit 1200) for 5 s, and by a 9 μm, 5 μm and 1 μm alumina slurry (Presi) on a cloth polishing pad for 10 min, 5 min and 3 min, respectively. Between each polishing step, the surfaces were cleaned in an ultrasonic ethanol bath (5 min) in order to remove any impurity. Finally, they were rinsed in an ultrasonic ultra pure water bath (5 min) and dried for 1 min using a N_2 stream.

The AuNPs–GC electrodes were obtained by CV scanning from open-circuit potential (*ca.* 0.9 V) to 0 V in a 0.1 M $NaNO_3$ deaerated solution containing 0.25 mM $HAuCl_4$ (pH 3) at a scan rate of 50 mV s^{-1} for a given number of scans (N). The resulting electrodes were activated in H_2SO_4 0.5 M by running 10 scans between 0.2 and 1.4 V at a scan rate of 100 mV s^{-1}. The analytical performances of AuNPs–GC electrodes towards Hg(II) detection were worse when this activation was not carried out.

Bare Au electrodes were polished successively by a 5 μm, 1 μm and 0.3 μm alumina slurry on a cloth polishing pad for 5 min, 3 min and 1 min, respectively. Between each polishing step, the electrodes were cleaned in an ultrasonic ethanol bath (5 min), and finally rinsed in an ultrasonic ultra pure water bath (5 min) and dried for 1 min using a N_2 stream. Au electrodes were then activated using the same conditions than for AuNPs–GC electrodes.

2.3. AuNPs characterization

The AuNPs–GC surface characterization was achieved by FEG-SEM using a JEOL JSM 6700F equipment with accelerating voltages of 5 and 10 kV and a working distance between 6 and 15 mm depending on the sample. Image analysis was carried out using MATLAB image processing toolbox software for particles counting (density estimation) and average diameter measurement. The den-

sity and average size of AuNPs were evaluated from a 12.1 μm^2 GC surface analysis (counting a minimum of 365 to 923 particles depending on the number of cyclic scans N). For each deposit, the error was calculated from the analysis of three different SEM images.

2.4. Stripping voltammetric detection of Hg(II)

Electrochemical detection and assay of Hg(II) on AuNPs–GC electrodes were performed in a deaerated 0.01 M HCl solution by using SWASV in the following conditions: cleaning potential = 0.8 V, cleaning time = 15 s; deposition cathodic potential = 0 V, deposition time (t_d) = 300 s; pulse amplitude = 25 mV, step amplitude = 5 mV, frequency = 200 Hz; anodic scan from 0 to 0.8 V. During the deposition step, the solution was stirred by means of the rotating working electrode (2000 rpm). A second scan was recorded immediately after the first one using the same conditions except t_d which was set to 30 s, and considered as a blank. Hg reoxidation peak heights were measured from the curves obtained after subtraction of the blank. This procedure, called "subtractive ASV method", has been previously reported in the literature [15]. It allows the analytical results to be freed from background vagaries (see Section 3 for further details). It is noteworthy that the subtractive anodic signals recorded with low Hg(II) concentrations were much noisier and we needed to use a Savitzky–Golay smoothing function.

3. Results and discussion

3.1. AuNPs electrodeposition on GC electrode

Fig. 1 shows the first two cyclic voltammograms obtained during the electroreduction of a 0.25 mM $AuCl_4^-$ solution in 0.1 M $NaNO_3$ on GC. In our study, GC was chosen as a chemically inert electrode material [53]. $NaNO_3$ was employed as supporting electrolyte instead of KCl because this latter has been reported to have a negative effect with respect to Au electrodeposition by favouring a coalescence phenomenon, leading to the formation of less numerous, large-sized NPs [54]. The shape of the first voltammogram (solid line) is consistent with that previously described under similar conditions [50,51]. The forward scan exhibits the reduction of Au(III) to Au(0) with a cathodic peak at 0.48 V, inducing the deposition of AuNPs onto the electrode surface. On the backward scan, a current crossover occurred at 0.62 V. Beyond this potential, the backward cathodic current became higher than the forward one. This is consistent with thermodynamics which predicts an easier growth of previously formed AuNPs than a nucleation of new AuNPs on GC electrode, because the deposition of gold requires less energy on gold than on GC [55,56]. On the second voltammogram (dashed line), the reduction peak of Au(III) was shifted from 0.48 to 0.78 V, strengthening that Au deposition occurred preferentially on the NPs created during the first scan. It is noteworthy that the current crossover observed on the first voltammogram is strongly dependent on the surface conditioning: systematically no crossover was observed when the electrode surface was not sufficiently polished (not shown). On the contrary, in the case of satisfactory electrode surface preparation, the crossover was observed, although not reported in some previous studies [57]. One has also to note the decrease of $AuCl_4^-$ cathodic peak current between the two voltammograms. This variation is mainly due to the consumption of $AuCl_4^-$ in the diffusion layer. As a matter of fact when the experiment was performed by stirring the solution during 1 min between the first and the second curves, the reduction peak recorded at the second scan was nearly as high as that of the first scan (not shown). For the following potential scans (i.e. from N = 2 to 20), only a slight decrease of the reduction peak current at 0.78 V was observed, and the peak potential slightly moved to less cathodic values. Some experiments were also performed using an $AuCl_4^-$ concentration of 1.0 mM, but they led to broad peaks with respect to Hg(0) oxidation. This is consistent with the observation that the most homogenous deposits have been obtained using low Au(III) concentrations around 0.1 mM [57,58]. For this reason, an $AuCl_4^-$ concentration of 0.25 mM was chosen in the subsequent studies.

3.2. Characterization of AuNPs

Several AuNPs–GC modified electrodes were elaborated using CV by varying the number of cyclic scans of the electrodeposition step from 1 to 20. The resulting modified electrodes were then characterized using CV in H_2SO_4 0.5 M. Fig. 2 shows the electrochemical response of the AuNPs–GC electrode scanning between 0.2 and 1.4 V, for four electrodeposition scans. The anodic peaks at 1.13 and 1.33 V were associated to Au oxidation. The presence of two peaks is indicative of the formation of several kinds of Au "oxides" resulting from a very complicated sorption mechanism of OH^- ions onto different crystallographic faces [51,59]. On the backward scan, the peak at 0.89 V corresponded to the subsequent reduction of the oxides previously formed.

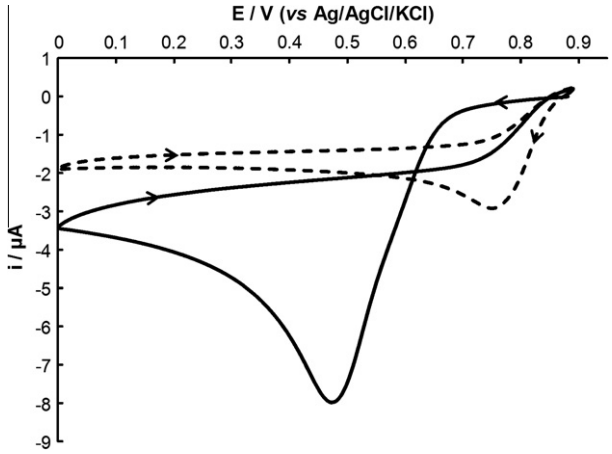

Fig. 1. CVs recorded during Au(III) electroreduction at a GC electrode in a 0.1 M $NaNO_3$ deaerated solution containing $HAuCl_4$ 0.25 mM: first (solid line) and second (dashed line) consecutive scans. Scan rate: 50 mV s^{-1}.

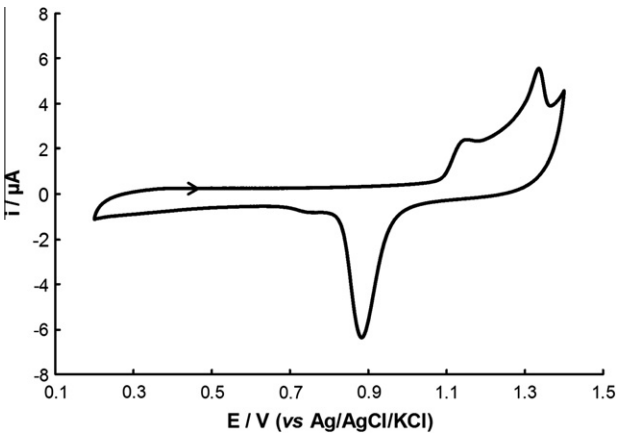

Fig. 2. CV recorded at a AuNPs–GC electrode (N = 4) in a 0.5 M H_2SO_4 solution. Scan rate: 100 mV s^{-1}.

Increasing N, the shape of the CVs remained unchanged, but all anodic (E_p = 1.13 and 1.33 V) and cathodic (E_p = 0.89 V) peak currents increased. Table 1 summarizes the data obtained concerning the charge consumed during Au electrodeposition step $Q_{Au(III)}$ on the one hand and the charge corresponding to Au oxides reduction Q_{oxides} in H_2SO_4 on the another hand. From these data, it can be clearly observed that both charges increase with N, i.e. the global amount of electrodeposited Au depends on the number of electrodeposition scans N. Moreover Q_{oxides} is strongly lower than $Q_{Au(III)}$ whatever N. Assuming that the faradic yield for Au electrodeposition is 100%, and that Q_{oxides} is similar to the charge consumed during the oxidation of AuNPs when plotting CVs in H_2SO_4, one can conclude that only the Au atom layers at the AuNPs–electrolyte interface are believed to be effectively oxidized.

Table 1
Characterization of AuNPs on GC and Δi_p of Hg(0) re-oxidation for different numbers of cyclic scans (N) during the electrodeposition step.

N	$Q_{Au(III)}$ (μC)[a]	Q_{oxides} (μC)[b]	NPs density (μm^{-2})[c]	Average diameter (nm)[c]	Δi_p (μA)[d]
1	99	2.7	53 ± 2	27 ± 16	5.0 ± 1.3
2	157	3.9	62 ± 4	36 ± 14	7.1 ± 0.3
3	195	4.1	60 ± 1	37 ± 15	7.4 ± 0.2
4	260	5.8	73 ± 3	36 ± 13	7.0 ± 0.4
8	437	9.4	64 ± 3	41 ± 15	6.5 ± 0.2
12	582	17	31 ± 1	63 ± 18	5.5 ± 0.5
16	682	18	27 ± 5	64 ± 19	5.0 ± 0.5
20	846	20	32 ± 2	71 ± 20	4.3 ± 0.2

[a] $Q_{Au(III)}$ is the charge consumed during the electroreduction step of $HAuCl_4$ 0.25 mM.
[b] Q_{oxides} is the charge corresponding to the reduction of Au oxides (peak at 0.89 V in Fig. 2) in H_2SO_4 0.5 M.
[c] See Section 2 for details on NPs density and average diameter estimation.
[d] Δi_p is the subtractive peak current of Hg(0) re-oxidation measured from a 4 nM Hg(II) solution (see Figs. 4 and 5).

In order to further characterize the AuNPs deposits, FEG-SEM analyses were carried out for six significant values of N (Fig. 3). The electrodeposited AuNPs can be separated into two distinct populations: the first one is related to small and spherical-shaped NPs and the second one to larger, aggregate-like NPs. The AuNPs density and size data obtained using FEG-SEM are reported in Table 1. An increase in the particle density as a function of N can be noticed up to four potential scans, then the density decreased down to 12 cycles and finally remained nearly constant till 20 scans. At the same time, the average size of the particles increased with respect to the number of cycles. This evolution of both the AuNPs density and the average size clearly illustrates a gradual coalescence phenomenon from N = 4. However, while increasing N between 1 and 4 scans, small, spherical-shaped NPs formation is favoured, and then the density reaches a critical value beyond which NPs begin to coalesce, leading to larger, less homogenously distributed NPs. In the latter case, a preferential growth of particles over the formation of new nucleation events takes place, in accordance with thermodynamics considerations previously discussed.

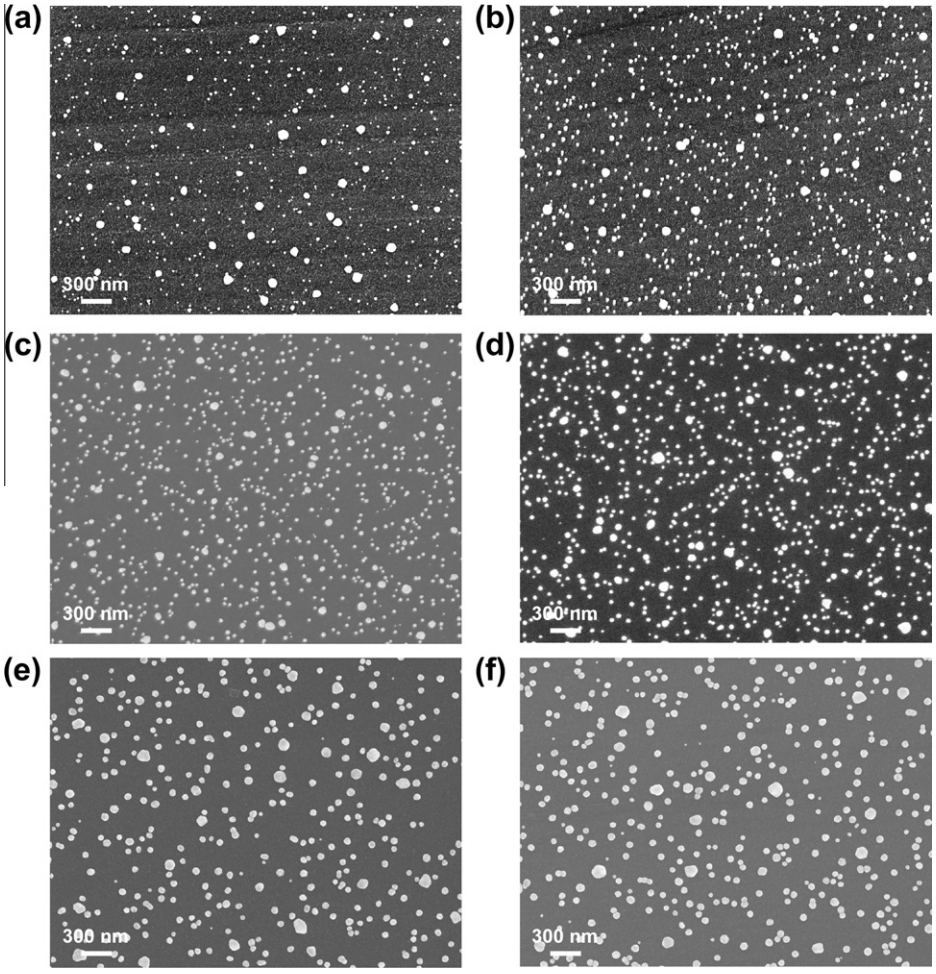

Fig. 3. FEG-SEM images of AuNPs–GC electrodes prepared by CV from a 0.25 mM $HAuCl_4$ solution in 0.1 M $NaNO_3$ (see Section 2 for conditions). Number of cyclic scans N: (a) 1; (b) 2; (c) 4; (d) 8; (e) 12; (f) 16.

3.3. Electrochemical response of Hg(II) at AuNPs–GC electrode

The electrochemical response of low Hg(II) concentrations at AuNPs–GC electrodes was examined using SWASV in a 0.01 M HCl solution. For preliminary experiments, a Hg(II) concentration higher than 1 nM was chosen because this value is easily detectable and low enough to allow further optimization of the system. HCl was chosen as the supporting electrolyte according to the literature, since many authors have reported an enhanced sensitivity with respect to Hg(II) trace detection while operating in the presence of some amount of Cl^- ions [17–19]. This medium rarely fits with real samples and could in a first approach limit the application fields of the proposed method, particularly for *in situ* analysis. However, these experimental conditions allow total Hg(II) speciation to be quantified. Fig. 4 shows the typical SWASV signals recorded at a AuNPs–GC electrode prepared using $N = 4$. The signal obtained in the case where $t_d = 300$ s (solid line) exhibited a typical broadened shape with a sharp, well-defined peak at 0.63 V, the latter one being associated to the oxidation of Hg(0) previously reduced on the AuNPs during the preconcentration step. It was checked that no peak was recorded at this potential while operating in the absence of Hg(II) during the preconcentration step (Fig. 4, dotted line). However, a higher baseline was recorded in this latter case. This broad baseline is well documented in the literature, both at solid Au electrode [19] and AuNPs [48], but the explanation remains still unclear and leads to extensive discussion. Taking into account the presence of a high concentration of Cl^- ions, some authors [19,48] proposed the formation of calomel during Hg(0) oxidation and its subsequent precipitation onto the electrode surface due to its poor solubility in water [34]. However, this statement is not supported by our observations while operating in the absence of Hg(II) into the solution. Indeed, the same broad background was observed, although a little higher, using a freshly prepared new electrode (Fig. 4, dotted line).

Finally, due to this broad baseline, Hg(0) reoxidation peak was expected to be difficult to extract for analytical purpose. To overcome this drawback and to obtain a suitable analytical blank, a procedure consisting in recording a SWASV using the same parameters than for Hg(II) analysis was established except for t_d that was set to 30 s. In these conditions, the voltammogram exhibited only a small shoulder in the potential region of Hg(0) oxidation (Fig. 4, dashed line). Such a procedure is commonly reported in the literature to be used as analytical blank [15,17,18]. The resulting signal Δi *vs.* E obtained by subtracting this blank to the voltammogram recorded for $t_d = 300$ s in the presence of Hg(II) is depicted in the inset of Fig. 4. We also verified that in the same experimental conditions, no response at all was observed on an unmodified GC electrode, and only a small, ill-defined peak was recorded on bare Au (not shown).

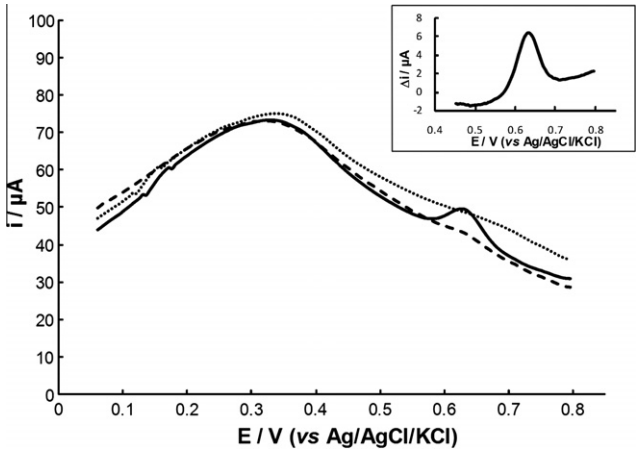

Fig. 4. Typical SWASV signals recorded at a AuNPs–GC electrode ($N = 4$) in a 0.01 M HCl solution containing Hg(II) 4 nM using $t_d = 300$ s (solid line) or $t_d = 30$ s (dashed line), and in the absence of Hg(II) using $t_d = 300$ s (dotted line). Inset: resulting signal after subtraction of dashed line from solid line.

3.4. Optimization of Hg(II) detection at AuNPs–GC electrodes

In order to optimize Hg(II) trace determination on AuNPs–GC electrodes, the influence of varying N on the electrochemical response of a 4 nM Hg(II) solution was examined (Fig. 5). A maximum was observed between $Q_{Au(III)} = 157$ µC ($N = 2$) and $Q_{Au(III)} = 260$ µC ($N = 4$). From the comparison of Fig. 5 with data in Table 1, it is noticeable that the peak current is correlated to both AuNPs density and size rather than to the global amount of electrodeposited Au, the highest current being recorded for a high density of small NPs (73 μm^{-2}). This result highlights the importance of a careful characterization of AuNPs deposit, especially in the case where the modified electrode is devoted to an analytical aim. To the best of our knowledge it is the first time that such a correlation between both AuNPs density and size and the analytical performances of the resulting modified electrode for Hg(II) detection is evidenced.

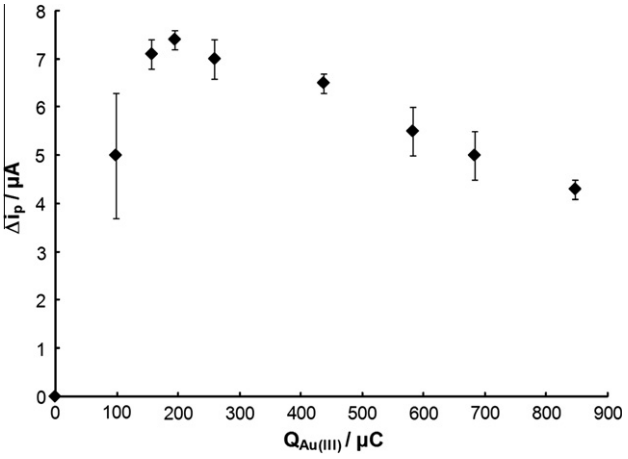

Fig. 5. Effect of the charge consumed during the electrodeposition of Au(III) on the peak current of Hg(0) re-oxidation (measured from a 4 nM Hg(II) solution in HCl 0.01 M). Three different measurements were performed for each value of $Q_{Au(III)}$.

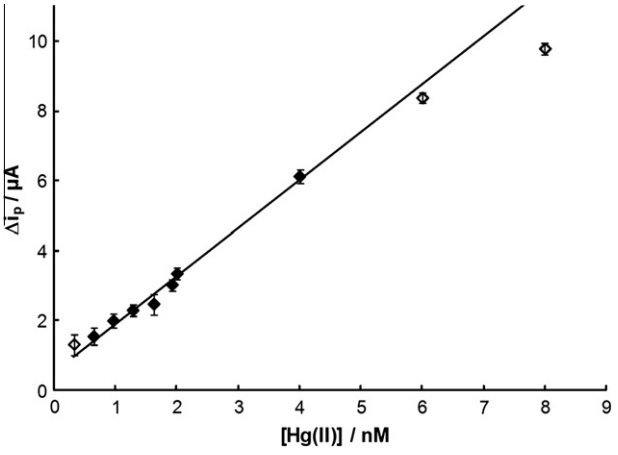

Fig. 6. Calibration curve obtained by SWASV on a AuNPs–GC electrode ($N = 4$) in a deaerated 0.01 M HCl solution. White-colored points were not included in the linear regression.

Table 2
Comparison of the experimental conditions and analytical performances of the different electrochemical sensors for Hg(II) detection based on electrodeposited AuNPs.

Substrate	Electrodeposition method	Average NPs diameter (nm)	Normalized sensitivity ($\mu A\ nM^{-1}\ min^{-1}$) [b]	LD (pM)	Ref.
Au	Chronoamperometry	30 ± 10	0.009	660	[49]
GC	Chronoamperometry	125 ± 25	0.652	7.5	[48]
GC/organic nanofibers	CV	120 [a]	0.962	40	[52]
GC	CV	36 ± 13	0.274	420	This work

[a] In this work, bimetallic Au–Pt NPs were used and AuNPs only were electrodeposited.
[b] The value of the normalized sensitivity was calculated by dividing the slope of the linear response by the preconcentration time. Hg(II) determination was performed using SWASV in each case.

3.5. Analytical performances for Hg(II) detection

Under the optimized experimental conditions (SWASV as described in Section 2, and $N = 4$), the analytical performances of the AuNPs–GC electrodes were examined. Fig. 6 shows the calibration curve obtained as a function of Hg(II) concentration. The AuNPs–GC electrode exhibited a good linearity in the range 0.64–4.00 nM (seven standard concentrations) with a correlation coefficient of 0.994. From the slope of the calibration plot, the sensitivity of the AuNPs–GC electrode was found to be 1.37 $\mu A\ nM^{-1}$ for $t_d = 300$ s. For Hg(II) concentration higher than 4 nM the slope decreased, probably due to a saturation phenomena of the accessible surface of AuNPs. This problem could be overpassed by decreasing the duration of the preconcentration step, for instance using a t_d value of 60 or 180 s. However, as our work aimed at determining very low concentrations, no further experiment was performed in that way. A limit of detection (LD) of 0.42 nM was calculated for a signal-to-noise ratio of 3 [60]. This LD is well below the guideline value provided by the World Health Organization (1 $\mu g\ L^{-1}$, *ca.* 5 nM) [61]. It could be significantly improved by increasing t_d. However, it is higher than that of all previously reported systems based on electrodeposited AuNPs (see Table 2). Particularly a pertinent comparison can be made with Abollino's et al. study [48] adopting similar experimental conditions and parameters optimization strategy, excepted that AuNPs have been electrodeposited in their case by constant potential electrolysis (−0.8 V *vs.* Ag/AgCl/KCl during 6 min). A LD more than 50 times lower than ours and a normalized sensitivity more than twice better were reported with a metal deposit looking like more a 3D porous nanostructured Au film than a AuNPs array. This result points out the influence of AuNPs electrodeposition mode and of the AuNPs structure on the analytical performances of the resulting modified electrodes.

4. Conclusion

In this work, we present for the first time AuNPs–GC electrodes prepared using CV for various numbers of electrodeposition scans *N*. Although not often used, CV proved to be an efficient mode for spherical-like shaped NPs electrodeposition. The systematic characterization of these electrodes using CV and FEG-SEM for different values of *N* allowed a correlation to be made between both AuNPs density and size and the performances of the electrode towards Hg(II) detection. AuNPs–GC electrodes exhibit interesting performances with respect to Hg(II) trace determination, and the best electrochemical responses were obtained for a high density (73 ± 3 particles μm^{-2}) of small NPs (36 ± 13 nm). From those observations, both NPs density and diameter appeared to be key features with respect to analytical performances. Using the optimal conditions ($N = 4$), the response of the AuNPs–GC electrode was linear in the range 0.64–4.00 nM, and the limit of detection was estimated to 0.42 nM. A careful comparison with the few other works dealing with electrodeposited AuNPs devoted to Hg(II) detection indicates that the choice of the electrodeposition method is important since it can give rise to different level of control of the AuNPs characteristics. To get further insight into the relationship between AuNPs characteristics and their analytical performances, future work will be devoted to perform a comparative study of different electrodeposition modes and their respective effect towards Hg(II) trace analysis.

Acknowledgments

This work was part of a project financially supported by the Foundation STAE (Sciences et Technologies pour l'Aéronautique et l'Espace) under the acronym "MAISOE" (Microlaboratoires d'Analyses *In Situ* pour des Observatoires Environnementaux). The authors thank Dr. Yannick Hallez and Dr. Jérémie Viguié for their help in MATLAB programming. The authors thank the referees for their fruitful comments.

References

[1] D.Q. Hung, O. Nekrassova, R.G. Compton, Talanta 64 (2004) 269–277.
[2] A. Bobrowski, A. Krolicka, J. Zarebski, Electroanalysis 21 (2009) 1449–1458.
[3] M. Korbas, S.R. Blechinger, P.H. Krone, I.J. Pickering, G.N. George, Proc. Natl. Acad. Sci. USA 105 (2008) 12108–12112.
[4] G.E. McKeown-Eyssen, J. Ruedy, A. Neims, Am. J. Epidemiol. 118 (1983) 470–479.
[5] I. Onyido, A.R. Norris, E. Buncel, Chem. Rev. 104 (2004) 5911–5930.
[6] J.R. Miller, J. Rowland, P.J. Lechler, M. Desilets, L.C. Hsu, Water Air Soil Pollut. 86 (1996) 373–388.
[7] F.M.M. Morel, A.M.L. Kraepiel, M. Amyot, Annu. Rev. Ecol. Syst. 29 (1998) 543–566.
[8] R. Eisler, Environ. Geochem. Health 25 (2003) 325–345.
[9] Q. Wang, D. Kim, D.D. Dionysiou, G.A. Sorial, D. Timberlake, Environ. Pollut. 131 (2004) 323–336.
[10] L. Laffont, J.E. Sonke, L. Maurice, H. Hintelmann, M. Pouilly, Y. Sanchez Bacarreza, T. Perez, P. Behra, Environ. Sci. Technol. 43 (2009) 8985–8990.
[11] K. Leopold, M. Foulkes, P. Worsfold, Anal. Chim. Acta 663 (2010) 127–138.
[12] H.M. Abu-Shawish, J. Hazard. Mater. 167 (2009) 602–608.
[13] D. Jagner, M. Josefson, K. Årén, Anal. Chim. Acta 141 (1982) 147–156.
[14] J. Wen, R.M. Cassidy, Anal. Chem. 68 (1996) 1047–1053.
[15] L. Sipos, H.W. Nürnberg, P. Valenta, M. Branica, Anal. Chim. Acta 115 (1980) 25–42.
[16] S. Meyer, F. Scholz, R. Trittler, Fresenius J. Anal. Chem. 356 (1996) 247–252.
[17] Y. Bonfil, M. Brand, E. Kirowa-Eisner, Anal. Chim. Acta 424 (2000) 65–76.
[18] P. Salaun, C.M.G. van den Berg, Anal. Chem. 78 (2006) 5052–5060.
[19] A. Giacomino, O. Abollino, M. Malandrino, E. Mentasti, Talanta 75 (2008) 266–273.
[20] K.Z. Brainina, N.A. Malakhova, N.Y. Stojko, Fresenius J. Anal. Chem. 368 (2000) 307–325.
[21] J.M. Pinilla, L. Hernandez, A.J. Conesa, Anal. Chim. Acta 319 (1996) 25–30.
[22] R. Fukai, L. Huynh-Ngoc, Anal. Chim. Acta 83 (1976) 375–379.
[23] D. Jagner, Anal. Chim. Acta 105 (1979) 33–41.
[24] J. Svarc-Gajic, Z. Stojanovic, Z. Suturovic, N. Marjanovic, S. Kravic, Desalination 249 (2009) 253–259.
[25] M. Shamsipur, J. Tashkhourian, B. Hemmateenejad, H. Sharghi, Talanta 64 (2004) 590–596.
[26] H. Yi, Anal. Bioanal. Chem. 377 (2003) 770–774.
[27] S.Y. Ly, S.K. Kim, T.H. Kim, Y.S. Jung, S.M. Lee, J. Appl. Electrochem. 35 (2005) 567–571.
[28] G.G. Muntyanu, J. Anal. Chem. 56 (2001) 546–551.
[29] P. Ugo, S. Zampieri, L.M. Moretto, D. Paolucci, Anal. Chim. Acta 434 (2001) 291–300.
[30] E.A. Viltchinskaia, L.L. Zeigman, D.M. Garcia, P.F. Santos, Electroanalysis 9 (1997) 633–640.
[31] L.A. Khustenko, L.N. Larina, B.F. Nazarov, J. Anal. Chem. 58 (2003) 262–267.

[32] S. Daniele, C. Bragato, M.A. Baldo, J. Wang, J. Lu, Analyst 125 (2000) 731–735.
[33] C. Garnier, L. Lesven, G. Billon, A. Magnier, O. Mikkelsen, I. Pizeta, Anal. Bioanal. Chem. 386 (2006) 313–323.
[34] O. Ordeig, C.E. Banks, J.d. Campo, F.X. Munoz, R.G. Compton, Electroanalysis 18 (2006) 573–578.
[35] P. Ugo, L. Sperni, L.M. Moretto, Electroanalysis 9 (1997) 1153–1158.
[36] K.-S. Yoo, S.-B. Woo, J.-Y. Jyoung, Bull. Korean Chem. Soc. 24 (2003) 27–31.
[37] . Colilla, M.A. Mendiola, J.R. Procopio, M.T. Sevilla, Electroanalysis 17 (2005) 933–940.
[38] J. Wu, L. Li, B. Shen, G. Cheng, P. He, Y. Fang, Electroanalysis 22 (2010) 479–482.
[39] D. Wu, Q. Zhang, X. Chu, H. Wang, G. Shen, R. Yu, Biosens. Bioelectron. 25 (2010) 1025–1031.
[40] C.M. Welch, R.G. Compton, Anal. Bioanal. Chem. 384 (2006) 601–619.
[41] M. Oyama, Anal. Sci. 26 (2010) 1–12.
[42] M. Grzelczak, J. Perez-Juste, P. Mulvaney, L.M. Liz-Marzan, Chem. Soc. Rev. 37 (2008) 1783–1791.
[43] Z. Wang, L. Ma, Coord. Chem. Rev. 253 (2009) 1607–1618.
[44] X. Zhou, Q. Wei, K. Sun, L. Wang, Appl. Phys. Lett. 94 (2009). 133107/133101–133107/133103.
[45] W. Abidi, H. Remita, Recent Patents Eng. 4 (2010) 170–188.
[46] X. Dai, O. Nekrassova, M.E. Hyde, R.G. Compton, Anal. Chem. 76 (2004) 5924–5929.
[47] U.S. Mohanty, J. Appl. Electrochem. 41 (2011) 257–270.
[48] O. Abollino, A. Giacomino, M. Malandrino, G. Piscionieri, E. Mentasti, Electroanalysis 20 (2008) 75–83.
[49] X.H. Gao, W.Z. Wei, L. Yang, T.J. Yin, Y. Wang, Anal. Lett. 38 (2005) 2327–2343.
[50] L. Komsiyska, G. Staikov, Electrochim. Acta 54 (2008) 168–172.
[51] A.P. O'Mullane, S.J. Ippolito, Y.M. Sabri, V. Bansal, S.K. Bhargava, Langmuir 25 (2009) 3845–3852.
[52] J. Gong, T. Zhou, D. Song, L. Zhang, X. Hu, Anal. Chem. 82 (2010) 567–573.
[53] K. Kinoshita, Carbon: Electrochemical and Physicochemical Properties, Wiley, New York, 1988.
[54] Y. Wang, J. Deng, J. Di, Y. Tu, Electrochem. Commun. 11 (2009) 1034–1037.
[55] G. Gunawardena, G. Hills, I. Montenegro, B. Scharifker, J. Electroanal. Chem. 138 (1982) 225–239.
[56] D. Grujicic, B. Pesic, Electrochim. Acta 47 (2002) 2901–2912.
[57] M.O. Finot, G.D. Braybrook, M.T. McDermott, J. Electroanal. Chem. 466 (1999) 234–241.
[58] C.M. Welch, O. Nekrassova, X. Dai, M.E. Hyde, R.G. Compton, ChemPhysChem 5 (2004) 1405–1410.
[59] H. Angerstein-Kozlowska, B.E. Conway, A. Hamelin, L. Stoicoviciu, Electrochim. Acta 31 (1986) 1051–1061.
[60] Analytical Methods Committee, Analyst 112 (1987) 199–204.
[61] Guidelines for Drinking-water Quality, third ed., vol. 1: Recommendations World Health Organization, Geneva, 2008 <http://www.who.int/water_sanitation_health/dwq/gdwq3rev/en/> (accessed 16.06.11).